Journal of Nuclear Materials 404 (2010) 82–96

Contents lists available at ScienceDirect

Journal of Nuclear Materials

journal homepage: www.elsevier.com/locate/jnucmat

Review

Models of liquid metal corrosion

J. Zhang *, P. Hosemann, S. Maloy

Decision and Application Division, Los Alamos National Laboratory, Los Alamos, NM 87544, United States

ARTICLE INFO

Article history:
Received 24 November 2009
Accepted 24 May 2010

ABSTRACT

In the present study, models for liquid metal corrosion are reviewed and their applications in nuclear reactor engineering are discussed. The paper presents mathematical analysis of liquid metal corrosion, including species transport in solid steels, in flowing liquid metals, and mass exchange at liquid/solid interface. The survey illustrates the mechanisms of the liquid metal corrosion and sets up a system to calculate the corrosion rate and to study the corrosion species distributions in the solid and liquid metal/alloys. Both light liquid metal/alloy (sodium and sodium–potassium) and heavy liquid metal/alloy (liquid lead and lead–bismuth) are considered. Oxygen effects on liquid metal corrosion are also discussed. For liquid sodium and sodium–potassium the corrosion rate increases with increasing oxygen concentration, while for liquid lead and lead–bismuth it is reasonable to produce a protective oxide layer using an oxygen control technique which can mitigate the corrosion rate significantly. Finally, the corrosion–oxidation interaction in liquid lead and lead–bismuth are discussed.

Contents

1. Introduction . . . 83
2. Liquid metal corrosion theory . . . 84
   2.1. Basic equations . . . 84
   2.2. Mass exchange at the solid/liquid interface . . . 84
   2.3. Corrosion rate for general cases . . . 84
      2.3.1. Cases with recession but no selective corrosion layer . . . 85
      2.3.2. Cases with diffusion layer only . . . 85
      2.3.3. Cases with both diffusion layer and surface recession . . . 85
   2.4. Boundary conditions for steady states . . . 85
3. Corrosion product transport in liquid phase (isothermal cases) . . . 85
   3.1. Mass transfer coefficient for fully developed turbulent flow . . . 85
   3.2. Transient corrosion cases . . . 86
4. Corrosion product transport in liquid phase (non-isothermal loop cases) . . . 87
   4.1. General description . . . 87
   4.2. Epstein's model . . . 87
   4.3. Sannier and Santarini's model . . . 88
   4.4. Kinetic corrosion model . . . 88
   4.5. Particulate model . . . 89
5. Transport in solid . . . 90
   5.1. Stoichiometric corrosion . . . 90
   5.2. Selective corrosion . . . 90
   5.3. Selective corrosion without surface recession . . . 90
   5.4. Corrosion with a constant surface corrosion rate . . . 91
   5.5. Two region problem . . . 92
      5.5.1. With zero surface recession rate . . . 92
      5.5.2. With constant surface recession rate . . . 92

* Corresponding author. Address: International and Nuclear System Engineering, MS K-575, Los Alamos National Laboratory, Los Alamos, NM 87544, United States. Tel.: +1 505 667 7444; fax: +1 505 665 2897.
E-mail address: jszhang@lanl.gov (J. Zhang).

0022-3115/$ - see front matter © 2010 Published by Elsevier B.V.
doi:10.1016/j.jnucmat.2010.05.024

6. Surface recession rate determination . . . 93
7. Oxygen effects on liquid metal corrosion . . . 93
7.1. Oxygen solubility . . . 93
7.2. Oxygen distribution coefficient . . . 93
7.3. Oxygen effects on corrosion by liquid sodium and NaK . . . 94
7.4. Oxygen effects on corrosion by liquid lead and LBE . . . 94
8. Models of corrosion–oxidation interactions in liquid lead and LBE with oxygen control . . . 94
9. Discussions . . . 95
10. Conclusions . . . 96
Acknowledgements . . . 96
References . . . 96

1. Introduction

Liquid metal corrosion is one of the key factors that have to be considered when using liquid metal as a heat transfer medium such as the primary coolant in advanced nuclear reactors. Liquid metal corrosion is a physical or physical–chemical process, involving species dissolution and transport, chemical reactions and new phase formation. The processes can be simply shown as in Fig. 1.

As shown in the figure, there are three significant steps: (1) transport in the solid (metal or alloy), (2) dissolution of the steel constituents into the liquid, or mass exchange at the solid/liquid interface, and (3) transport of the corrosion products and impurities in the liquid. The first step is governed by the movability of mass in the solid materials, and the second step is governed by dissolution/chemical reactions at the liquid/solid interface, while the third step is controlled by both mass convection and diffusion in the liquid. The transport processes in liquid and solid are coupled with each other at solid/liquid interface through mass exchange. The two processes (transports in liquid and solid) can also lead to impurity redistribution and new phase formation at the surface area of the solid contacting with the liquid metal. The impurities redistribution and new phase formation also relate to the surface behaviors as shown in Fig. 1.

The transport of the corrosion products in the liquid metal and their reactions with impurities play important roles in liquid metal corrosion. The mass transfer has been classified into two categories [1]: dissimilar metal mass transfer and thermal gradient mass transfer. The first one is due to the thermodynamic requirement that all element chemical potentials should be equivalent in all phases, and the second one is due to the temperature dependent solubility in the liquid of all corrosion products.

In an isothermal liquid metal closed loop system, if the loop is made of same materials the corrosion may finally stop because of saturation of the corrosion products, while in a non-isothermal system such as the primary coolant loop system of a nuclear reactor, the final state is a kinetic equilibrium in which the amount of corrosion is balanced by the amount of the precipitation all through the loop. It is the precipitation that sustains the corrosion in a non-isothermal liquid metal loop [2]. The precipitating corrosion product may be in the form of layers tightly adhering on the pipe wall or particles suspending in the liquid [3]. The second form may inhibit the corrosion when the particles are transported to corrosion sections where they dissolve again, however, the two-phase flow with solid particles results in mechanical erosion which can damage the structural materials seriously.

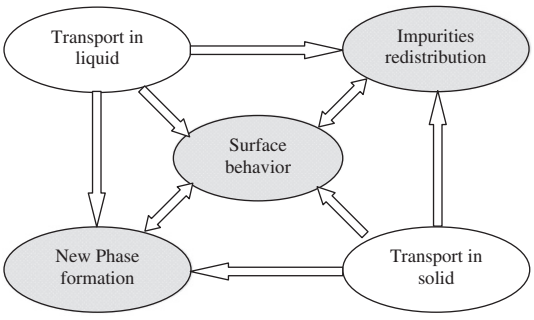

Fig. 1. Simple view of corrosion by liquid metal.

Liquid metal corrosion may or may not result in surface recession of structural materials, depending on the transport of corrosion product in the solid and liquid phases, and the dissolution reaction at the interface. The slower rate of the mass transfer rate in the liquid and the dissolution rate (reaction rate) at the interface controls the whole corrosion rate. If the corrosion rate is controlled by mass transfer rate, it is called as mass transfer controlled corrosion, and for the other case, it is called as activation controlled or dissolution controlled corrosion. If the diffusion rate in the solid is fast enough to balance the mass transfer rate, there will be no surface recession. However, such ideal case does not occur in a practical system because the diffusion in the solid phase is always the slowest process. Since different constituents have different diffusion coefficients in the steel, a selective corrosion layer can be formed due to selective corrosion if the diffusion rate in the steel is not very low compared with the dissolution rate at interface [4].

Liquid metal corrosion depends on the liquid metal itself and impurities in it. Liquid sodium and sodium–potassium alloy are less corrosive than liquid lead and lead–bismuth alloy at the same operating conditions when impurities' effects are not considered. If liquid lead or lead–bismuth is selected for the primary coolant of nuclear reactors, protective methods must be applied to mitigate the corrosion of structural materials. One of these methods is oxygen control technique which can control the oxygen concentration in the liquid in a certain range to form a protective oxide layer on structural material surfaces and to avoid the precipitation of the lead oxide from the liquid [5]. For liquid sodium and sodium–potassium alloy, the oxygen concentration has to be controlled as low as possible because the corrosion rate by liquid sodium and sodium–potassium increases significantly with oxygen concentration [6].

Liquid metal corrosion involves many physical and chemical processes: mass diffusion and convection, oxidation, impurity redistribution, liquid metal penetration, etc. In the present survey, some of these processes are considered mathematically. Theoretical models and analytical solutions of the liquid metal corrosion are reviewed, compared and analyzed. The models for different steps of liquid metal corrosion are integrated into one theoretical model system based on mass exchange at the solid/liquid interface by chemical and physical processes of liquid metal corrosion.

2. Liquid metal corrosion theory

2.1. Basic equations

Concentration in mass fraction is denoted by c. The following parameters are first defined:

c'_i = concentration in liquid;
$c'_{i,s}$ = solubility in liquid;
$c'_{i,I}$ = concentration at the interface in liquid side;
$c'_{i,b}$ = bulk concentration in liquid;
c_i = concentration in solid;
$c_{i,0}$ = bulk or initial concentration in solid;
$c_{i,I}$ = concentration at the interface in solid side.

The subscript i represents the species i. Generally, the mass transfer equation can be written by:

$$\frac{\partial c}{\partial t} + \nabla J + q = 0 \tag{1}$$

where q is the homogeneous reaction term in the material bulk and J is the flux. For species i in liquid:

$$J'_i = -D'_i \nabla c'_i + \vec{u} c'_i \tag{2}$$

where $\vec{u}$ is the velocity vector and D'_i is the diffusion coefficient in the liquid. For the species i in solid with a corrosion rate $R(t)$ as function of time and with the original point fixed on the surface of the solid materials as shown in Fig. 2.

The mass flux can be expressed by:

$$J_i = -D_i \nabla c_i + R(t) c_i \tag{3}$$

where D_i is the diffusion coefficient of species i in the solid. The mass transport equation in the coordinate for constant diffusion coefficient can be expressed by:

$$\frac{\partial c'_i}{\partial t} + u\frac{\partial c'_i}{\partial x} + v\frac{\partial c'_i}{\partial y} + w\frac{\partial c'_i}{\partial z} = D'_i\left(\frac{\partial^2 c'_i}{\partial x^2} + \frac{\partial^2 c'_i}{\partial y^2} + \frac{\partial^2 c'_i}{\partial z^2}\right) + q'_i \tag{4}$$

for the species in liquid ($y > 0$, Fig. 2), where u, v, and w are the velocity components in x, y, z direction, and:

$$\frac{\partial c_i}{\partial t} + R(t)\frac{\partial c_i}{\partial y} = D_i\left(\frac{\partial^2 c_i}{\partial x^2} + \frac{\partial^2 c_i}{\partial y^2} + \frac{\partial^2 c_i}{\partial z^2}\right) + q_i, \tag{5}$$

in solid ($y < 0$). The diffusion coefficient in liquid and solid are assumed to be independent of the space all through the paper. If the reaction term is greater than zero, the reaction is species production, while if the reaction term is less than zero, the reaction is species consumption.

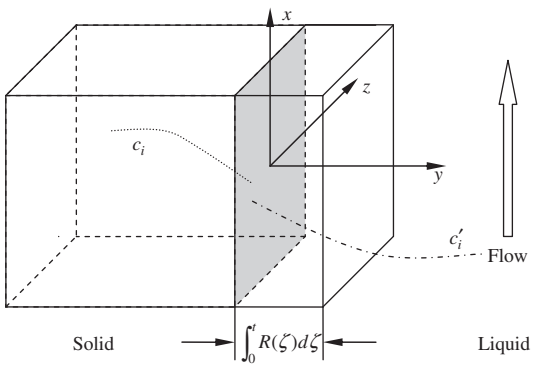

Fig. 2. Coordinate of the corrosion by liquid metal.

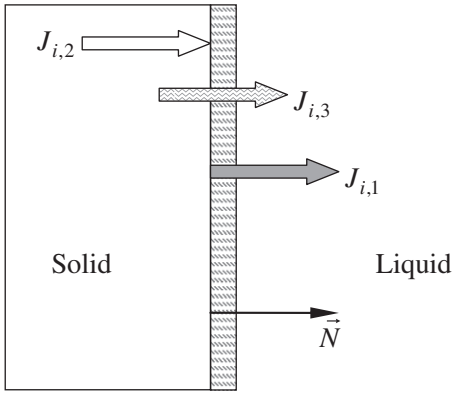

Fig. 3. Mass fluxes at solid/liquid interface.

2.2. Mass exchange at the solid/liquid interface

At the interface along the normal direction, as shown in Fig. 3 there are (a) mass flux in the liquid, $J_{i,1}$; (b) mass flux in the solid, $J_{i,2}$ and (c) mass flux through the interface due to absorption and desorption, $J_{i,3}$. The fluxes are defined by:

$$J_{i,1} = -\rho_L D'_i \frac{\partial c'_i}{\partial \vec{N}} + \rho_L R c'_{i,I} \tag{6}$$

$$J_{i,2} = -\rho_S D_i \frac{\partial c_i}{\partial \vec{N}} + \rho_S R c_{i,I} \tag{7}$$

$$J_{i,3} = \rho_S k_d c_{i,I} - \rho_L k_a c'_{i,I} \tag{8}$$

where

ρ_L = density of the liquid;
ρ_S = density of the solid;
k_a = absorption rate;
k_d = desorption rate;

and $\vec{N}$ is the normal as shown in Fig. 3. In Eqs. (6)–(8), the reaction terms are neglected.

The concentration at the interface in both solid and liquid sides is governed by:

$$\frac{dc'_{i,I}}{dt} = J_{i,3} - J_{i,1} \tag{9}$$

in liquid and

$$\frac{dc_{i,I}}{dt} = J_{i,2} - J_{i,3} \tag{10}$$

in solid. Considering a steady state or a quasi-steady state at the surface, we get:

$$J_{i,1} = J_{i,2} = J_{i,3} \tag{11}$$

Therefore, the transports in liquid and solid are coupled to each other through mass balance at the interface.

2.3. Corrosion rate for general cases

At the beginning for a fresh liquid, the dissolution reaction will be the fast step among the three steps and the control step of the net corrosion will be the third step: mass transfer in the liquid. While for long term operations at a steady state the net corrosion will be controlled by either dissolution at the surface (activation control) or mass transfer in liquid (mass transfer control). For the mass transfer control, if the diffusion flux of the corrosion product in solid is less than the mass transfer rate in liquid, dissolution of

the surface will meet up the difference resulting in a finite surface recession rate (second term in Eq. (7)). The recession rate (R) is generally called the bulk corrosion rate or corrosion rate in the present study. If the diffusion flux through the interface is no less than the mass transfer rate, there will be no bulk corrosion or surface recession, and all the corrosion products come from the species diffuses in the solid (all the terms in Eqs. (6) and (7) related to R will not appear in the equations). For cases with very high flow velocity, the corrosion rate becomes independent of the flow velocity and the corrosion becomes activation control which is controlled by the dissolution reaction. If the diffusion rate in the solid is greater than the dissolution rate, then there is no surface recession, otherwise there will be surface recession.

Although the diffusion in solid is the slowest process among the three steps of the liquid metal corrosion, it can result in a selective corrosion layer at the surface contacting with the liquid because of the different diffusion coefficients of the steel constituents in the steel. This selective corrosion changes the steel composition at the surface area, which can lead to material failure. If the diffusion rate in the solid is very low compared to the dissolution rate at the surface, the diffusion layer or the selective corrosion layer can be avoided. For such cases, all the corrosion products entering into the liquid are from the dissolution of the surface or the surface recession.

2.3.1. Cases with recession but no selective corrosion layer

For such cases, the first term on the right of Eq. (7) is zero. Equalizing the expressions on the right of Eqs. (6) and (7), the bulk corrosion rate can be expressed by:

$$R = -\frac{\rho_L}{\rho_S - \rho_L \sum_i c'_{i,I}} \sum_i D'_i \frac{\partial c'_i}{\partial \vec{N}} \tag{12}$$

If the concentration of corrosion products in liquid at the liquid/solid interface is assumed to be very small, Eq. (12) can be simplified to:

$$R = -\frac{\rho_L}{\rho_S} \sum_i D'_i \frac{\partial c'_i}{\partial \vec{N}} \tag{13}$$

Then the weight loss rate can be obtained by:

$$R_{\Delta w} = R\rho_S \tag{14}$$

2.3.2. Cases with diffusion layer only

In these cases, the diffusion in the solid is fast enough to supply the mass removal by the liquid metal. Therefore, there will be no surface recession, and the bulk corrosion rate is zero ($R = 0$, no surface recession). The weight loss can be obtained by:

$$R_{\Delta w} = -\rho_L \sum_i D'_i \frac{\partial c'_i}{\partial \vec{N}} \tag{15}$$

2.3.3. Cases with both diffusion layer and surface recession

In these cases, the diffusion rate in the solid is pretty large, but is less the mass transfer rate. There will be surface recession in this case. The recession rate can be calculated through the mass balance at the interface. The rate can be expressed by:

$$R = -\frac{\rho_L}{\rho_S - \rho_L \sum_i c'_{i,I}} \left(\sum_i D'_i \frac{\partial c'_i}{\partial \vec{N}} - \frac{\rho_S}{\rho_L} \sum_i D_i \frac{\partial c_i}{\partial \vec{N}} \right) \tag{16}$$

The weight loss rate can be obtained by:

$$R_{\Delta w} = R\left(\rho_S - \rho_L \sum_i c'_{i,I} \right) \tag{17}$$

If we assume that $\sum_i c'_{i,I} \ll 1$, the weight loss rate can be simplified to:

$$R_{\Delta w} = R\rho_S \tag{18}$$

which is same to the case surface with recession only (Eq. (14)).

2.4. Boundary conditions for steady states

The metal dissolution reaction at solid/liquid interface can be represented by:

$$M_i(s) \Longleftrightarrow M_i(L) \tag{19}$$

There is an up limit of the concentration that may be either the solubility or the equilibrium concentration of the dissolved metal. If the dissolution reaction (Eq. (19)) is very fast, the concentration at the interface in the liquid reaches the limited concentration very quickly, and then at the steady state, the boundary concentration in the liquid phase can be expressed by:

$$c'_{i,I} = c'_{i,eq} \tag{20}$$

where $c'_{i,eq}$ is constant for a given operating condition. Based on this boundary equation, the flux $J_{i,1}$ can be calculated by solving the transport equation in the liquid phase. Then the boundary condition for the transport equation in the solid phase can be obtained through Eq. (9), and at a steady state the boundary condition can be expressed by:

$$D_i \frac{\partial c_i}{\partial \vec{N}} = R c_{i,I} - \frac{1}{\rho_S} J_{i,1} \tag{21}$$

which corresponds to a constant flux for the transport in the solid.

If the mass transfer in the liquid is very fast and can almost remove all corrosion products due to dissolution reaction, the concentration at the interface in solid phase will reach its limit value. Then boundary condition for a steady state of the transport equation in the solid phase can be expressed by:

$$c_{i,I} = c_{i,eq} \tag{22}$$

Similarly, for this case, the boundary condition for the transport equation in the liquid phase can be obtained through Eq. (9) and can be can expressed by:

$$D'_i \frac{\partial c'_i}{\partial \vec{N}} = R c'_{i,I} - \frac{1}{\rho_L} J_{i,2} \tag{23}$$

In which $J_{i,2}$ is known by solving the transport equation in the solid phase based on boundary condition of Eqs. (22). Eq. (23) corresponds to a constant flux boundary condition for the transport equation in the liquid phase.

3. Corrosion product transport in liquid phase (isothermal cases)

3.1. Mass transfer coefficient for fully developed turbulent flow

For a fully developed turbulent flow, the species concentration profile in the liquid can be simply shown as in Fig. 4. The variation of the concentration only occurs within the mass transfer boundary layer, while in the bulk flow, it can be assumed to be uniform. Based on this and assuming that the concentration has a linear distribution in the boundary layer as shown in the figure, the mass transfer coefficient in liquid is defined by

$$K_{i,m} = \frac{D'_i}{\delta_{i,m}} \tag{24}$$

$\delta_{i,m}$ is the thickness of the linear boundary layer. The mass transfer coefficient is a function of Reynolds number (Re) and

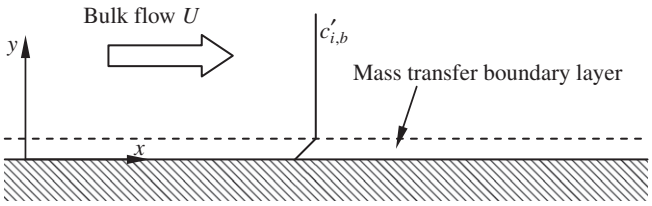

Fig. 4. Simple view of the concentration profile in turbulent flow.

Schmidt number (Sc) defined by: $\mathrm{Re} = dU/\upsilon$ and $Sc_i = \upsilon/D'_i$, where d is the hydraulic diameter and υ is the viscosity of the liquid. Conventionally, a dimensionless parameter, Sherwood number (Sh) is introduced by:

$$Sh_i = \frac{K_{i,m}d}{D'_i} \tag{25}$$

The Sherwood number can be expressed in terms of Reynolds number and Schmidt number by:

$$Sh_i = a\mathrm{Re}^b Sc_i^c \tag{26}$$

where a, b and c are constant and can be obtained theoretically [7] and experimentally [8–10]. Recommended relations are given in Table 1. The correlation by Pinczewski and Siderman is a theoretical result for high Schmidt number, and others are experimental correlations. The table indicates that the mass transfer coefficient depends on the Schmidt number with a power around 0.33 and Reynolds number with a power around 0.9.

Based on the definition of the mass transfer coefficient for fully developed turbulent flow, the mass transfer rate $J_{i,1}$ can be roughly rewritten by:

$$J_{i,1} = \rho_L K_{i,m}\left(c'_{i,I} - c'_{i,b}\right) + \rho_L R c'_{i,I} \tag{27}$$

where $c'_{i,b}$ is the concentration of corrosion products in bulk flow, which may be unknown variable and in some cases it is reasonable to assume it to be zero.

3.2. Transient corrosion cases

For a static case, there is no convection. The transport in the liquid metal is due to diffusion only. Considering a sample with an area A contacting with the liquid metal having a volume V, the concentration in the liquid, as a function of the exposure time, can be expressed by [3]:

$$\frac{dc'_i}{dt} = \alpha\lambda\left(c'_{i,eq} - c'_i\right) \tag{28}$$

where α is the specific dissolution rate, and λ is the ratio of the area A to the volume V, i.e. $\lambda = A/V$. By integrating Eq. (28), it is easy to get a solution as:

$$c'_i = c'_{i,eq}[1 - \exp(-\alpha\lambda t)] \tag{29}$$

To calculate the concentration, the dissolution rate α has to be determined first. For the mass transfer controlled corrosion, the dissolution rate depends on the diffusion coefficient [3] through:

Table 1
Correlations for Sherwood number.

$Sh = a\mathrm{Re}^b Sc^c$			
a	b	c	Ref.
0.0165	0.860	0.33	Berger and Hsu [8]
0.0177	0.875	0.296	Silverman [9]
0.0096	0.913	0.346	Harriott and Hamilton [10]
0.0102	0.90	0.33	Pinczewski and Sideman [7]

$$\alpha = kD'^n_i \tag{30}$$

where k and n are constant. For the activation controlled corrosion, the dissolution rate is independent of the diffusion coefficient and can be expressed by:

$$\alpha = 10^{a+b/T} \tag{31}$$

where a and b are constant and can be determined through experiments, for example, it was reported [11] that $a = -0.007$ and $b = -2388$ for dissolution rate (cm/s) in liquid sodium.

The weight loss rate can be obtained through the Eqs. (30) and (31):

$$R_{\Delta W_i} = \rho_L c'_{i,eq}\exp(-\alpha\lambda t) \tag{32}$$

Eq. (29) indicates that the concentration in the liquid increases with time and approaches the equilibrium concentration for long-term operation. Eq. (32) indicates that the corrosion rate or weight loss rate decreases with time and approaches zero. The change of the concentration and the corrosion rate with time shows that the corrosion stops if the exposure time is long enough.

It is necessary to notice that this model for corrosion in static liquid metal is based on the assumption that the concentration in the bulk liquid is uniform which is not true in practice. The concentration is not uniform at short-term and there is diffusion in the bulk liquid which affects the corrosion rate as function of time. However, with time elapsing, the concentration becomes uniform in the bulk liquid.

For a flow system, the convection has to be considered. Considering a two dimensional channel flow as shown in Fig. 4, the length L is much larger than the hydraulic diameter d, so the diffusion term in the stream wise is much smaller than the diffusion term in the transverse direction, while the transverse flow velocity is much smaller than the stream wise velocity and its effect on convection can be neglected. Then the transport equation can be simply written as:

$$\frac{\partial c'_i}{\partial t} + u\frac{\partial c'_i}{\partial x} = D'_i\frac{\partial^2 c'_i}{\partial^2 y} \tag{33}$$

In which the reaction term in the flow is also neglected. For liquid metals, the Schmidt number is very large, leading to a fact that the mass transfer boundary layer is underneath the linear momentum boundary [2], therefore in the mass transfer boundary layer the flow velocity can be expressed by a linear function as $u = \gamma y$ with the shear stress rate $\gamma = fU^2/2\upsilon$ in which the friction factor f depends on Reynolds number [12]:

$$f = 0.079\mathrm{Re}^{-0.25} \quad \text{for } 2.3\times10^3 < \mathrm{Re} < 10^5$$
$$f = 0.046\mathrm{Re}^{-0.2} \quad \text{for } \mathrm{Re} \geqslant 10^5$$

Introducing the following non-dimensional parameters:

$$\eta = \left(\frac{\gamma}{D'_i d}\right)^{1/3} y, \quad \xi = \frac{x}{d}, \quad \tau = \left(\frac{d^2}{\gamma^2 D'_i}\right)^{-1/3} t$$

Eq. (33) becomes

$$\frac{\partial c'_i}{\partial \tau} + \eta\frac{\partial c'_i}{\partial \xi} = \frac{\partial^2 c'_i}{\partial^2 \eta} \tag{34}$$

For constant concentration at the boundary, Soliman and Chambre [13] obtained a solution of the time dependent corrosion rate:

$$J_{i,1}/J_{i,1,ss} = 1 + 3^{1/3}\Gamma\left(\frac{1}{3}\right)\sum_{n=1}^{\infty}\frac{1}{s_n} \times \exp\left[-\frac{2}{27}(s_n\tau)^3\right]Ai\left[\left(\frac{s_n\tau}{3^{2/3}}\right)^2\right] \tag{35}$$

$J_{i,1,ss}$ is the corrosion rate at the steady state:

$$J_{i,1,ss} = \rho_L c'_{i,I} \frac{3^{1/3}}{\Gamma(1/3)} \left(\frac{\gamma D_i'^2}{\xi d}\right)^{1/3} \tag{36}$$

$\Gamma()$ is Gamma function defined by:

$$\Gamma(x) = \int_0^\infty e^{-t} t^{x-1}\, dt \tag{37}$$

and Ai() is the Airy function defined by:

$$\mathrm{Ai}(x) = 3^{-2/3} \sum_{n=0}^{\infty} \frac{1}{n!} \sin[2/3(n+1)\pi] \times \int_0^\infty z^{n/3-2/3} e^{-z}\, dz (3^{1/3}x)^n \tag{38}$$

and s_n are constant:

$$s_{1-6} = (2.33810, 4.08794, 5.52055, 6.7867, 7.9441, 9.0227) \tag{39}$$

and for $n \geqslant 7$

$$s_n = \left[\frac{3\pi}{8}(4n-1)\right]^{2/3} \tag{40}$$

For short-term exposure ($\tau \to 0$), Eq. (35) reduces to:

$$J_{i,1}/J_{i,1,ss} \sim \frac{1.0480}{\tau^{1/2}} \tag{41}$$

and for long term exposure ($\tau \to \infty$), Eq. (35) reduces to:

$$J_{i,1}/J_{i,1,ss} \sim 1 + \frac{3^{2/2}\Gamma(\frac{1}{3})}{2\sqrt{\pi} s_1} \frac{1}{(s_1\tau)^{1/2}} \exp\left[-\frac{4}{27}(s_1\tau)^3\right] \tag{42}$$

The transient corrosion rate in an isothermal system is shown in Fig. 5. As shown in the figure, the rate decreases and it almost reaches the steady state value when $\tau = 1.0$. The short-term solution can be applied up to $\tau = 1.0$, while the long-term solution is valuable when τ is no less than 1.2. For estimating the true time needed for corrosion to reach the value of steady state, the dimensionless time is rewritten as:

$$\tau = \left(\frac{4}{f^2}\frac{Sc}{\mathrm{Re}}\right)^{-1/3} \frac{d}{U} t \tag{43}$$

For iron in lead [14], $Sc = 333.0$ at temperature 500 °C. Considering $\mathrm{Re} = 10^5$ and $U = 2.0$ m/s, the time for reaching the steady state is about 4.0 min which is very short compared with several years operation of a nuclear reactor. For other liquid metals such as Lead–bismuth and sodium, similar result will be obtained. Therefore, the transient effects can be neglected for liquid metal corrosion.

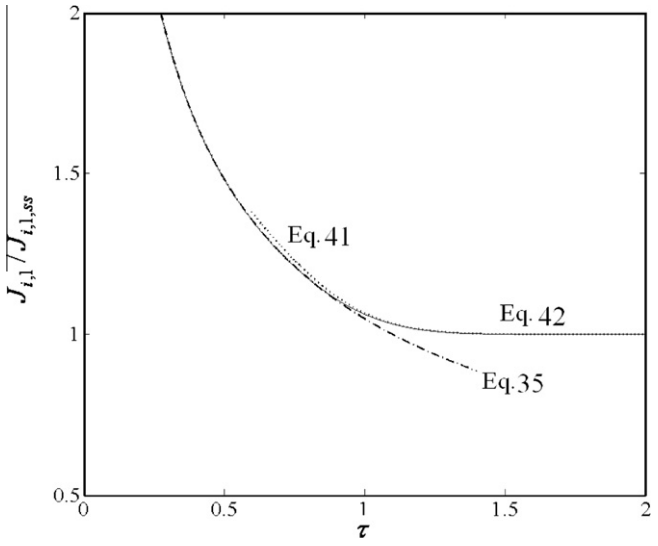

Fig. 5. Cure of transient corrosion rate as a function of dimensionless time.

4. Corrosion product transport in liquid phase (non-isothermal loop cases)

4.1. General description

Non-isothermal liquid metal loops have been used as the primary coolant loop of a liquid metal cooled fast reactor. For such a system, the liquid metal passes through the reactor core and reaches its highest temperature at the outlet of the core, and then passes through a heat exchanger where its temperature is reduced to its lowest temperature. It is the temperature gradient along the flow path that sustains the corrosion/precipitation process in such non-isothermal loop. In this section, we consider cases with time-independent concentration distribution at the inner surface along the stream wise direction.

If the non-isothermal loop is made of one kind of steel, thermal gradient mass transfer will be the main corrosion mechanism which is because of temperature dependent solubility of the steel constituents in the liquid metal. Considering that liquid metal is not being refreshed during operation for a liquid metal nuclear coolant system, the total amount of corrosion should equal the total amount of precipitation all through the loop. The corrosion and precipitation zones can be predicted by a theoretical model [14]. It is reported that the highest corrosion rate occurs at the core outlet, and highest precipitation rate happens at the outlet of the heat exchanger.

4.2. Epstein's model

Epstein [3] considered an idealized loop with a structure having a hot isothermal zone, a cool isothermal zone, a heat exchanger and a heater.

For the mass transfer corrosion, the wall concentration at the hot zone equals the equilibrium concentration of the species in the liquid at the highest temperature, while the bulk concentration in the liquid is assumed to be the equilibrium concentration at the lowest temperature all over the loop. Therefore, at the hot zone:

$$c'_{i,I} - c'_{i,b} = c'_{i,eq}(T = T_{\max}) - c'_{i,eq}(T = T_{\min}) = \frac{dc'_{i,eq}}{dT}\Delta T \tag{44}$$

where ΔT is the temperature difference in the loop: $\Delta T = T_{\max} - T_{\min}$. The corrosion rate at the hot zone was obtained by:

$$J_{i,1}(T = T_{\max}) = \rho_L K_{i,m}(T = T_{\max}) \frac{dc'_{i,eq}}{dT}\Delta T \tag{45}$$

Replace the mass transfer coefficient using the theoretical expression given in Table 1, to obtain:

$$J_{i,1}(T = T_{\max}) = 0.0102 \rho_L \mathrm{Re}^{0.9} Sc^{1/3} \frac{D_i'}{d} \frac{dc'_{i,eq}}{dT}\Delta T \tag{46}$$

Eq. (46) indicates that the loop length has no effects on the corrosion rate at the hot zone and the corrosion rate has a same value along the hottest zone, and there is only one systematic parameter, ΔT, that affects the corrosion rate. Eq. (46) cannot predict the downstream effects which have been reported experimentally [15]. On the other hand, Eq. (46) can only be applied to a loop with small temperature difference considering Eq. (44).

Commonly, the equilibrium concentration equals the solubility which can be expressed by:

$$c'_{i,eq} = 10^{A+B/T} \tag{47}$$

where A and B are constant. Substitute the solubility expression into Eq. (46), the corrosion rate at the hottest temperature isothermal zone in a non-isothermal loop can be obtained:

$$J_{i,1}(T = T_{\max}) = 0.0102\rho_L \mathrm{Re}^{0.9} Sc^{1/3} \frac{D'_i}{d} 10^{A+B/T} \frac{-B\Delta T}{T^2_{\max}} \tag{48}$$

Eq. (48) indicates that the corrosion rate increases with the temperature gradient and the maximal temperature increasing.

For activation controlled corrosion, the concentration in the bulk liquid is governed by:

$$\frac{dc'_{i,b}}{dx} = \kappa\left(c'_{i,s} - c'_{i,b}\right) \tag{49}$$

where $\kappa = 4\alpha/dU$. Epstein [3] assumed that the corrosion rate at the hot zone can be expressed by:

$$J_{i,1}(T = T_{\max}) = \frac{1}{4} d\rho_L U \left(\frac{dc'_{i,b}}{dx}\right)_{\max} \tag{50}$$

and can be rewritten in the following formation if ζ is the value of x at which $dc'_{i,b}/dx$ is a maximum:

$$J_{i,1}(T = T_{\max}) = \frac{1}{4} d\rho_L U \bar{\kappa}(c'_{i,s}(\zeta) - c'_{i,b}(\zeta)) \tag{51}$$

where: $c'_{i,b}(x) = \exp(-\bar{\kappa}x)[I(x) + \overline{C}]$ and $I(x) = \bar{\kappa}\int c'_{i,s}(x)\exp(\bar{\kappa}x)dx$. ζ and the integral constant $\overline{C}$ are determined by:

$$\left(\frac{dc'_{i,s}}{dx}\right)_{x=\zeta} = \bar{\kappa}\left\{c'_{i,s}(\zeta) - \exp(-\bar{\kappa}\zeta)[I(\zeta) + \overline{C}]\right\} \tag{52}$$

$$(\exp(-\bar{\kappa}L) - 1)\overline{C} = \exp(-\bar{\kappa}L)I(L) - I(0) \tag{53}$$

The bar in Eqs. (51)–(53) represents the value at the medium temperature.

4.3. Sannier and Santarini's model

Sannier and Santarini developed a corrosion model for liquid lead loops. The model can predict both corrosion and deposition in a closed loop system [16]. The corrosion products' transport in the liquid was classed into three steps: dissolution at the interface, diffusion through the boundary layer, and convection in the bulk flow:

Convection rate in the bulk flow:

$$J_{i,1,conv} = \frac{Ud}{4}\frac{dc'_{i,b}}{dx} \tag{54}$$

Diffusion rate through the boundary layer:

$$J_{i,1,diff} = \frac{D'_i}{\delta_D}\left(c'_{i,I} - c'_{i,b}\right) \tag{55}$$

where δ_D is the mass transfer boundary layer related to the flow.

Dissolution rate at the interface:

$$J_{i,1,diss} = \frac{k_d}{c'_{i,s}}\left(c'_{i,s} - c'_{i,I}\right) \tag{56}$$

Parameters are defined as: $k_d = k_{d0}\exp(-h_d/RT)$, $c'_{i,s} = c'_{i,s,0}\exp(-\beta/RT)$, where k_d is in m/s.

Case I: *activation control* $(U = \infty,\ D'_i = \infty)$

For such case, the convection transport rate through the bulk flow and diffusion transport rate through diffusion boundary layer are much greater than the dissolution rate at the interface, i.e. $J_{i,1,conv} \gg J_{i,1,diss}$, $J_{i,1,diff} \gg J_{i,1,diss}$, therefore:

$$c'_{i,b} \approx c'_{i,I}, \quad J_{i,1} = \rho_L J_{i,1,diss} \tag{57}$$

Rewrite Eq. (56), one gets:

$$J_{i,1} = \rho_L k_{d0}\exp\left(-\frac{h_d}{RT}\right) - \frac{k_{d0}}{c'_{i,s,0}}\rho_L c'_{i,b}\exp\left(\frac{\beta - h_d}{RT}\right) \tag{58}$$

The bulk concentration is determined by considering

$$J_{i,1} = J_{i,1,conv} \tag{59}$$

at the steady state and the mass conservation equation shown in Eq. (54).

Case II: *convection* control $(k_d = \infty,\ D'_i = \infty)$

In this case, the dissolution rate at the interface and the diffusion rate through the diffusion boundary layer, i.e. $J_{i,1,diff} \gg J_{i,1,conv}$, $J_{i,1,diss} \gg J_{i,1,conv}$, the corrosion rate is determined by the convection rate in the bulk flow:

$$c'_{i,b} \approx c'_{i,I} \approx c'_{i,s}, \quad J_{i,1} = \rho_L J_{i,1,conv} \tag{60}$$

The corrosion rate can be expressed by:

$$J_{i,1} = \rho_L \frac{\beta dU c_{i,,s,0}}{RT^2}\frac{dT}{dx}\exp\left(-\frac{\beta}{RT}\right) \tag{61}$$

Case III: *diffusion* control ($U = \infty$, $k_d = \infty$)

In this case, the convection rate in the bulk flow and the dissolution rate at the interface are much greater than the diffusion rate through the boundary layer, i.e. $J_{i,1,conv} \gg J_{i,1,diff}$, $J_{i,1,diss} \gg J_{i,1,conv}$, therefore:

$$c'_{i,I} \approx c'_{i,s} \quad J_{i,1} = \rho_L J_{i,1,diff} \tag{62}$$

Considering that $D'_i = D'_{i,0}\exp(-E_D/RT)$, the Eq. (62) can be rewritten by:

$$J_{i,1} = \rho_L \frac{D'_{i,0}c'_{i,s,0}}{\delta}\left[\exp\left(-\frac{E_D - \beta}{RT}\right) - \frac{c'_{i,b}}{c'_{i,s,0}}\exp\left(-\frac{E_D}{RT}\right)\right] \tag{63}$$

Case IV: *Mixed corrosion mechanism*

A general relation for the corrosion rate determined in the liquid phase as:

$$\frac{d}{dx}\left[\left(\frac{1}{v_{diss}} + \frac{1}{v_{diff}}\right)J_{i,1}\right] + \frac{1}{v_{conv}}J_{i,1} - \frac{dc'_{i,s}}{dx} = 0 \tag{64}$$

where

$$v_{diss} = \frac{k_d}{c'_{i,s}}, \quad v_{diff} = \frac{D'_i}{\delta}, \quad v_{conv} = \frac{Ud}{4}$$

In a non-isothermal loop, v_{diss} and v_{diff} are function of x, and v_{conv} may or may not be the function of x depending on the flow path and the hydraulic diameter of the flow path.

4.4. Kinetic corrosion model

For studying the corrosion by heavy liquid metal such as liquid lead and lead bismuth, He and Li [2] developed a kinetic model by solving Eq. (34) at a steady state. The model was extended and applied by Zhang and Li in series publications [17]. First of all, it is assumed that the concentration at the pipe wall (liquid/solid interface) does not depend on time and its distribution along the flow direction can be expended in a Fourier series:

$$c'_{i,I}(\xi) = \sum_k a_k \exp(2\pi i k \xi) \tag{65}$$

Then, the concentration distribution in the mass transfer boundary layer is obtained as:

$$c'_{i,s}(\eta,\xi) = a_0 + \sum_{k>0} Y_k(\eta) e^{2\pi k i \xi} + \sum_{k<0} \overline{Y}_{|k|}(\eta) e^{2\pi k i \xi} \tag{66}$$

and the corrosion flux through the boundary layer is expressed by:

$$\begin{aligned} J_{i,1}(\xi) &= -\rho_L D'_i \frac{\partial c'_i}{\partial y}_{y=0} \\ &= 0.3825 \rho_L \frac{D'_i}{d}\left(\frac{d}{L}\right)^{1/3} Sc^{1/3} \mathrm{Re}^{0.6} \sum_{k\neq 0} Q_k \exp(2\pi k i \xi) \end{aligned} \tag{67}$$

where

$$Y_{k>0}(\eta) = \frac{a_k}{Ai(0)} Ai((2\pi k i)^{1/3}\eta)$$
$$Y_{k<0}(\eta) = \overline{Y}_{|k|}(\eta)$$
$$Q_{k>0} = a_k k^{1/3} i^{1/3}$$
$$Q_{k<0} = a_k |k|^{1/3} (-i)^{1/3}$$

The concentration of corrosion products in the bulk flow is also obtained:

$$c'_{i,b}(\xi) = c'_{i,b,0} + 0.3825 \frac{LP}{A}\left(\frac{d}{L}\right)^{1/3} Sc^{-2/3} \mathrm{Re}^{-0.4} \sum_{k\neq 0} \beta_k \exp(2\pi k i \xi) \tag{68}$$

where $c'_{i,b,0}$ is the average bulk concentration calculated by considering the amount of corrosion has to be balanced with the amount of precipitation in a closed non-isothermal loop which can be expressed by:

$$\int_0^L J_{i,1}(x) P(x) dx = 0 \tag{69}$$

P is the wetted perimeter. The coefficient β_k in Eq. (68) relates to Q_k through:

$$\beta_k = Q_k/(2\pi k i), \quad \text{for } k>0; \quad \beta_k = \bar{\beta}_{-k}, \quad \text{for } k<0; \quad \text{and} \quad \beta_0 = 0$$

For activation controlled corrosion, $c'_{i,b} = c'_{i,I}$, and $c'_{i,b}$ is governed by Eq. (49) which can be rewritten in the following formation:

$$q_L \frac{dc'_{i,b}(\xi)}{d\xi} = P(\xi)\alpha(\xi)\left[c'_{i,s}(\xi) - c'_{i,b}(\xi)\right] \tag{70}$$

where $q_L = UA$ (A is the flow area) is the liquid flow rate. For a closed loop system, q_L is constant. Integrate Eq. (70), the solution is obtained as:

$$c'_{i,b}(\xi) = e^{-\phi(x)}[I(\xi) + G] \tag{71}$$

with

$$\phi(\xi) = \int \frac{P(\xi)}{q_L}\alpha(\xi) d\xi$$
$$I(\xi) = \int \frac{P(\xi)}{q_L}\alpha(\xi) c'_{i,s}(\xi) e^{\phi(\xi)} d\xi$$

and G is an integration constant which can be determined by the condition $c'_{i,b}(0) = c'_{i,b}(1)$.

To get a solution with an expression similar to Eq. (67), a new variable is introduced:

$$\zeta = \phi(\xi) \tag{72}$$

and a constant is defined by:

$$l = \int_0^1 P(\tau)\alpha(\tau)/q_L d\tau \tag{73}$$

Then Eq. (70) becomes:

$$\frac{dc'_{i,b}(\zeta)}{d\zeta} = c'_{i,s}(\zeta) - c'_{i,b}(\zeta) \tag{74}$$

Expand the bulk concentration into the following Fourier series:

$$c'_{i,b}(\zeta) = \sum_k c_k \exp[2ik\pi\zeta/l] \tag{75}$$

and also the solubility:

$$c'_{i,s}(\zeta) = \sum_k b_k \exp[2ik\pi\zeta/l] \tag{76}$$

For a non-isothermal loop, if the temperature profile is given, b_k can be calculated. Substitute Eqs. (76) and (75) into Eq. (74), and the $c_k$in Eq. (75) can be expressed by:

$$c_k = \frac{b_k(1 - 2\pi k i/l)}{1 - 4k^2\pi^2/l^2} \tag{77}$$

Therefore the solution of the bulk concentration is

$$c'_{i,b}(\xi) = \sum_k \frac{b_k(1 - 2\pi k i/l)}{1 - 4k^2\pi^2/l^2} \exp[2\pi k i \phi(\xi)/l] \tag{78}$$

and the corrosion/deposition rate as a function of the stream wise coordinate:

$$J_{i,1}(\xi) = \rho_L \alpha(\xi) \sum_k \frac{b_k(2\pi k i/l - 4\pi^2 k^2/l^2)}{1 - 4\pi^2 k^2/l^2} \exp[2\pi k i \phi(\xi)/l] \tag{79}$$

Clearly, the corrosion rate is also a function of the stream wise coordinate similar to the cases of mass transfer control.

There are some other models not listed in this survey, such as the models given in Refs. [18,19]. In Ref. the bulk concentration was assumed to be the average concentration of wall and the boundary layer thickness effects were considered in Ref. [19].

4.5. Particulate model

The corrosion product dissolved into the liquid metal in a non-isothermal loop can come out of the liquid as shown by the kinetic model. The products can come out in several formations such as suspending particles or as a deposit layer adhered on the wall surface. If the particles are small enough to remain in suspension, they can be transported to the corrosion section by the liquid and redissolve, which can inhibit the corrosion [3]. Therefore, most of the corrosion models for liquid metal corrosion not considering the coming out particles transport predict a higher corrosion rate compared with experimental data. The particulate model was first developed by Wachtel et al. [20] and then analyzed by Polley and Skyrme [6] and Weeks and Isaacs [21].

For diffusion controlled mass transfer, Polley and Skyrme [6] gave a Sherwood number for the particle that can dissolve into the liquid:

$$Sh_{i,p} = \frac{d_{i,p}K_{i,p}}{D'_i} = 2 + \varepsilon \mathrm{Re}_p^2 Sc^{1/3} \tag{80}$$

for the range of $1 \leqslant Sc \leqslant 1500$. The subscript p represents the parameter for the considered particle. ε is constant and is assumed to be less than unity. By rewriting Eq. (80), the mass transfer coefficient through the boundary layer around the particle can be expressed by:

$$K_{i,p} = \frac{D'_i}{d_{i,p}}\left(2 + \varepsilon \mathrm{Re}_p^2 Sc^{1/3}\right) \tag{81}$$

For particles of radius less than one micron under turbulent flow with $Re \leqslant 10^5$, the second term on the right side in Eq. (81) can be neglected. Then the equation becomes:

$$K_{i,p} \approx \frac{2D'_i}{d_{i,p}} \tag{82}$$

which indicates that the smaller the radius of the particle is, the faster the rate of the mass transfer will be. Physically, this means that smaller particles respond more rapidly to the turbulence so that mass transfer is dominated by diffusion rather than by convection [6]. The dissolution rate of the particle at the corrosion zones can be expressed by:

$$J_{i,p} = \rho_L K_{i,p}\left(c'_{i,sa} - c'_{i,b}\right) \tag{83}$$

$c'_{i,sa}$ is the saturation concentration in the fluid adjacent to the particle. Considering the Kelvin relationship [22], $c'_{i,sa}$ is related to the solubility through:

$$c'_{i,sa}(T) = c'_{i,s}(T)\exp\left(\frac{4\chi_i M_i}{d_p \rho_i RT}\right) \tag{84}$$

where χ_i is the metal i–liquid interface energy and M_i is the atomic weight of the metal i.

Assuming that the particle has a uniform distribution, the mass transport equation in the bulk liquid can be expressed by:

$$\rho_L UA\frac{dc'_{i,b}}{dx} = PJ_{i,1} + A\pi d_p^2 nJ_{i,p} \tag{85}$$

where n is the particle number in a unit volume. Substitute $J_{i,1} \approx \rho_L K_{i,m}\left(c'_{i,s} - c'_{i,b}\right)$ for mass transfer control and Eq. (83) into Eq. (85), it is gotten:

$$UA\frac{dc'_{i,b}}{dx} = PK_{i,m}\left(c'_{i,s} - c'_{i,b}\right) + A\pi d_p^2 nK_{i,p}\left(c'_{i,sa} - c'_{i,b}\right) \tag{86}$$

It should be noticed that for a given non-isothermal system, $K_{i,m}$, $c'_{i,s}$, $c'_{i,sa}$ are known, $K_{i,p}$ is related to the particle diameter which is governed by [6]:

$$\frac{dd_p}{dx} = \frac{4D'_i}{U\rho_i d_p}\left(c'_{i,b} - c'_{i,sa}\right) \tag{87}$$

For applications of the particular model, the particle concentration, particle size and distribution must be known.

5. Transport in solid

5.1. Stoichiometric corrosion

For such case, all the constituents of the solid materials dissolve into the liquid homogeneously, so the weight loss as a function of time can be expressed by:

$$\frac{d\Delta w}{dt} = \sum_i J_{i,\Delta w} \tag{88}$$

where $J_{i,\Delta w}$ is the weight loss of constituent i, and it is related to the net weight loss rate of the solid by [23]:

$$J_{i,\Delta w} = c_{i,0}\frac{d\Delta w}{dt} \tag{89}$$

where $c_{i,0}$ is the initial concentration of species i in the solid steel/alloy. Considering in the liquid side in an isothermal case, Eq. (88) can be simply rewritten:

$$\frac{d\Delta w}{dt} = \rho_L \alpha_{ste}\left(c_{ste,s} - c'_{ste,b}\right) \tag{90}$$

with α_{ste} is the dissolution rate of the steel, $c_{ste,s}$ and $c'_{ste,b}$ are the solubility of the steel in the liquid and the bulk concentration of the steel in the liquid. For a static system, the concentration in the bulk liquid is a function of time. The solution is given by Eq. (32). For a flowing system, it is reasonable to assume that $c'_{ste,b}$ is independent of the time but a function of the coordinate in the streamwise direction. Then Eq. (88) becomes:

$$\frac{d\Delta w}{dt} = \rho_L \alpha_{ste} c_{ste,s}\exp\left(-\frac{P\alpha_{ste}}{AU}x\right) \tag{91}$$

Instead of using weight loss rate for corrosion, select the surface recession rate to represent the corrosion rate, it is gotten [24]:

$$R_{ste} = \sum_i R_i c_{i,I} = \sum_i R_{ste} c_{i,0} \tag{92}$$

where R_{ste} is the corrosion rate of the steel and R_i is the corrosion rate of the species i. Therefore, knowing the actual species concentration at the interface and the original composition of the steel, one can estimate the pure species dissolution rate by:

$$R_i = R_{ste} c_{i,0}/c_{i,I} \tag{93}$$

5.2. Selective corrosion

The selective corrosion is due to the different diffusion rates of the steel constituents. In the case of selective corrosion, the weight of one constituent does not follow Eq. (89), that is:

$$J_{i,\Delta w} \neq c_{i,0}\frac{d\Delta w}{dt} \tag{94}$$

According to Ref. [23], the constituent is named by "noble" element if

$$J_{i,\Delta w} < c_{i,0}\frac{d\Delta w}{dt} \tag{95}$$

and "active" element if

$$J_{i,\Delta w} > c_{i,0}\frac{d\Delta w}{dt} \tag{96}$$

For the noble element, the initial corrosion rate is less than the rate dictated by its bulk fraction in the steel (Eq. (95)). For an active element, the initial corrosion rate is larger than the rate dictated by its bulk fraction (Eq. (96)), the mass initially corroding above stoichiometric amounts must come from within the steel by diffusion toward the liquid/solid interface.

For selective corrosion, the constituent concentration in the solid phase has to follow the following equation everywhere [23]:

$$\sum_i c_i = 1 \tag{97}$$

5.3. Selective corrosion without surface recession

Considering the diffusion term in the normal direction of liquid/solid interface, the governing equation of the species diffusion in the solid becomes:

$$\frac{\partial c_i}{\partial t} = D_i\frac{\partial^2 c_i}{\partial y^2} \tag{98}$$

For a constant concentration case at the surface (corresponding to a fast mass transfer in liquid phase), the boundary and initial conditions are:

$$c_i = c_{i,0} \quad \text{at } y < 0 \quad \text{for } t = 0 \tag{99a}$$

$$c_i = c_{i,I} \quad \text{at } y = 0 \quad \text{for } t > 0 \tag{99b}$$

$$c_i = c_{i,0} \quad \text{at } y \to -\infty \tag{99c}$$

With these conditions, the solution of Eq. (98) is:

$$c_i(y,t) = c_{i,I} + (c_{i,I} - c_{i,0})erf\left(\frac{y}{2\sqrt{D_i t}}\right) \tag{100}$$

where *erf*() is the error function. The weight loss rate is obtained by:

$$R_{i,\Delta w} = \rho_S(c_{i,0} - c_{i,I})\left(\frac{D_i}{\pi t}\right)^{1/2} \tag{101}$$

Then the weight loss per unit area is obtained by:

$$\Delta w_i = \int_0^t R_{i,\Delta w} dt = 2\rho_S(c_{i,0} - c_{i,I})\left(\frac{D_i t}{\pi}\right)^{1/2} \tag{102}$$

The total weight loss can be expressed by:

$$\Delta w = \sum_{i=1}^{N} \Delta w_i \tag{103}$$

where N is the total number of corrosion species. For particular cases $c_{i,I} = 0$, Eqs. (100) and (101) become:

$$c_i(y,t) = -c_{i,0} erf\left(\frac{y}{2\sqrt{D_i t}}\right) \tag{104}$$

$$\Delta w_i = \int_0^t R_{i,\Delta w}\, dt = 2\rho_S c_{i,0}\left(\frac{D_i t}{\pi}\right)^{1/2} \tag{105}$$

Eqs. (104) and (105) was first obtained and discussed by Anno and Walowit [25].

For a constant mass flux at the surface (corresponding to a constant concentration at the interface in liquid phase), the initial and boundary conditions are:

$$c_i = c_{i,0} \quad \text{at } y < 0 \quad \text{for } t = 0 \tag{106a}$$

$$-D_i\frac{\partial c_i}{\partial y} = J_{i,2} \quad \text{at } y = 0 \quad \text{for } t > 0 \tag{106b}$$

$$c_i = c_{i,0} \quad \text{at } y \to -\infty \tag{106c}$$

where $J_{i,2}$ is a constant which can be obtained by solving mass transfer equation in the liquid phase. Using these conditions, the solution of Eq. (98) is:

$$c_i(y,t) = c_{i,0} - \frac{2J_{i,2}}{\sqrt{D_i\pi}} t^{1/2}\left[\exp\left(\frac{-y^2}{4D_i t}\right) - \frac{y\pi^{1/2}}{2\sqrt{D_i t}} erfc\left(\frac{y}{2\sqrt{D_i t}}\right)\right] \tag{107}$$

Then the concentration at the interface is expressed by:

$$c_{i,I} = c_{i,0} - \frac{2J_{i,2}}{\sqrt{D_i\pi}} t^{1/2} \tag{108}$$

Considering that $c_{i,I} \geqslant 0$, Eqs. (108) and (107) can only be applied to time rage of $t < t_0$, where:

$$t_0 = \left(\frac{c_{i,0}\sqrt{D_i\pi}}{2J_{i,2}}\right)^2 \tag{109}$$

When $t \geqslant t_0$, $c_{i,I} = 0$.

5.4. Corrosion with a constant surface corrosion rate

With a constant recession rate, the governing equation for the transport in the solid phase can be expressed by:

$$\frac{\partial c_i}{\partial t} + R\frac{\partial c_i}{\partial y} = D_i\frac{\partial^2 c_i}{\partial y^2} \tag{110}$$

For the boundary condition indicated in Eq. (99), the solution was given by Ref. [23] as:

$$c_i = c_{i,0} - \frac{1}{2}(c_{i,0} - c_{i,I})\left[erfc\left(-\frac{\eta-\tau}{2\sqrt{\tau}}\right) + \exp(\eta) erfc\left(-\frac{\eta+\tau}{2\sqrt{\tau}}\right)\right] \tag{111}$$

where $\tau = R^2 t/D_i$, $\eta = Ry/D_i$. If $c_{i,I}$=0, Eq. (111) reduces to the solution obtained by Anno and Walowit [25]. The weight loss rate can be obtained by:

$$J_{i,2} = -\rho_S D_i\frac{\partial c_i}{\partial y}|_{y=0} + \rho_S R c_{i,I} = \frac{1}{2}\rho_s R(c_{i,0} - c_{i,I})\left[\frac{2}{\sqrt{\pi\tau}}\exp\left(-\frac{\tau}{4}\right) + erfc\left(-\frac{1}{2}\sqrt{\tau}\right)\right] + R\rho_S c_{i,I} \tag{112}$$

Integrate Eq. (112), the weight loss as a function of time is obtained:

$$\Delta w_i = \frac{1}{2}\rho_s D_i(c_{i,0} - c_{i,I})\left[\frac{2}{R} erf\left(\frac{\tau}{2}\right) + \frac{\tau}{R} erfc\left(-\frac{\tau}{2}\right) + \frac{2\tau}{R\sqrt{\pi}}\exp\left(-\frac{\tau^2}{4}\right)\right] + \frac{D_i}{R}\rho_S c_{i,I}\tau \tag{113}$$

For long-term operation or for the steady state, $t \to \infty$, Based on Eqs. (111)–(113):

$$c_i \to c_{i,0} - (c_{i,0} - c_{i,I})\exp(\eta) \tag{114a}$$

$$J_{i,2} \to \rho_S R c_{i,0} \tag{114b}$$

$$\Delta w_i \to \rho_S R c_{i,0} t \tag{114c}$$

Eq. (114) indicates that weight loss is determined by the surface recession rate and the bulk species content in the steel.

The curve of the weight loss as a function of time is given in Fig. 6. The total weight loss increases with time and has a linear dependence of time after τ = 2.0 which is the steady state relationship between the weight loss and the time as shown in Eq. (114c). According to this figure and considering the definition of non-dimensional time τ, the real time needed to reach the steady state can be estimated by the following equation:

$$t_0 \approx \frac{2D_i}{R^2} \tag{115}$$

Therefore, the higher the corrosion rate by the liquid is, the shorter the time for reaching the steady state will be.

For the boundary condition expressed by Eq. (106), the solution was obtained by Polley [26]:

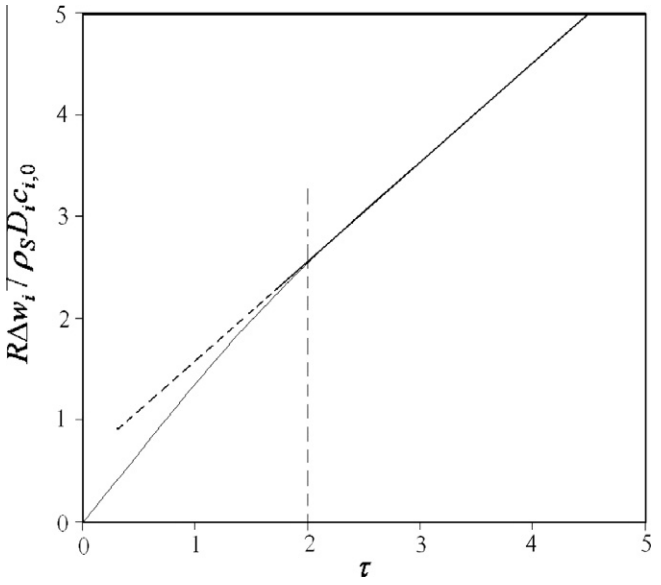

Fig. 6. Weight loss as a function of time, the surface concentration is set to be half of the bulk concentration in the steel.

$$c_i = c_{i,0} - \frac{1}{2}(c_{i,0} - c_{i,e})\left[erfc\left(-\frac{\eta-\tau}{2\sqrt{\tau}}\right) + \frac{1}{2}\exp(\eta)erfc \times \left(-\frac{\eta+\tau}{2\sqrt{\tau}}\right) - \frac{3}{2}\exp(-\eta+2\tau)erfc\left(-\frac{\eta-3\tau}{2\sqrt{\tau}}\right)\right] \quad (116)$$

with $c_{i,e} = J_{i,2}/\rho_s R$, and $J_{i,2}$ can be obtained by solving the transport equation in the liquid phase.

At the steady state, the solution becomes:

$$c_i = c_{i,0} - \frac{1}{2}(c_{i,0} - c_{i,e})\exp(\eta) \quad (117)$$

And the surface concentration can be calculated by:

$$c_{i,I} = \frac{1}{2}c_{i,0} + \frac{J_{i,2}}{\rho_s R} \quad (118)$$

5.5. Two region problem

5.5.1. With zero surface recession rate

When the constituents of initially austenitic steel are depleted by corrosion process beyond a specific minimum threshold level, the depleted layer becomes ferritic, which has been reported in liquid sodium experimentally [25].

In this section, we will consider the two-region problem with zero surface recession rate, i.e. $R = 0$. The coordinate and the profile for the active species are shown in Fig. 7. In the figure, $c_{i,a}$ and $c_{i,f}$ represent the concentration in austenitic phase and ferric phase, respectively, $c_{i,a,I}$ and $c_{i,f,I}$ represent the concentration at the austenite/ferrite interface, $y = -Y(t)$, where $Y(t)$ is the thickness of the ferric layer. For getting an analytic solution, it is assumed that the concentration is continuous at austenite/ferrite interface and the ferrite thickness follows the parabolic law. Furthermore, the concentration at the austenite/ferrite interface is also assumed to be a constant with time. Then

$$c_{i,a,I} = c_{i,f,I} = c_c \quad (119a)$$

$$Y(t) = (2k_p t)^{1/2} \quad (119b)$$

The other conditions are given by:

$$D_{i,a}\frac{\partial c_{i,a}}{\partial y} = D_{i,f}\frac{\partial c_{i,f}}{\partial y}, \quad \text{at } y = -Y(t) \quad (120a)$$

$$c_{i,a} \to c_{i,0}, \quad \text{when } y \to -\infty, \quad (120b)$$

$$c_{i,f} = c_{i,I}, \quad \text{at } y = 0, \quad (120c)$$

With these conditions, solutions for the concentration profile in the two phases were given by Anno and Walowit [25]:

$$c_{i,f} = c_{i,I} + \frac{c_c - c_{i,I}}{erf(\alpha)}erf\left[\frac{y}{2(D_{i,f}t)^{1/2}}\right] \quad (121)$$

$$c_{i,a} = c_{i,0} + \frac{c_0 - c_c}{erf\left(\alpha\left(\frac{D_{i,f}}{D_{i,a}}\right)^{1/2}\right)}erf\left[\frac{y}{2(D_{i,a}t)^{1/2}}\right] \quad (122)$$

where α is related to the parabolic constant k_p by:

$$k_p = 2\alpha^2 D_{i,f} \quad (123)$$

Following the analysis by Anno and Walowit, it will show that $\alpha \approx 1.0$. Then the interface concentration c_c can be calculated by considering the boundary condition (120a) at the ferrite/austenite interface:

$$\frac{c_{i,0} - c_c}{c_c} = \frac{e}{erf(1)}\left(\frac{D_{i,f}}{D_{i,a}}\right)^{1/2}\frac{erfc\left[\left(\frac{D_{i,f}}{D_{i,a}}\right)^{1/2}\right]}{\exp\left(-\frac{D_{i,f}}{D_{i,a}}\right)} \quad (124)$$

Considering that the nickel diffusion coefficient in ferrite is 5.5 time than that in austenite [25], that is $D_{Ni,f}/D_{Ni,a} = 5.5$, for Nickel we get:

$$c_c = 0.37c_{Ni,0} \quad (125)$$

5.5.2. With constant surface recession rate

For such a case, the coordinate and the concentration distribution is given in Fig. 8. It is impossible to get the transient analytical solution when both the ferric layer and the surface recession are presented in the problem, but it is possible to get the steady state species concentration in the solid. For a constant surface recession rate, the ferric layer is assumed following the Tedmon's equation [27]:

$$\frac{dY}{dt} = \frac{k_p}{Y} - R \quad (126)$$

with an initial condition:

$$Y = 0 \quad \text{when } t = 0 \quad (127)$$

The solution of Eq. (126) with the initial condition of Eq. (127) was obtained by Tedmon as:

$$t = -\frac{Y}{R} - \frac{k_p}{R^2}\ln\left(1 - \frac{R}{k_p}Y\right) \quad (128)$$

with an asymptotic thickness Y_0:

$$Y_0 = \frac{k_p}{R} \quad (129)$$

Considering that the formation of the ferric layer is due to the depletion of nickel in the steel, the following equation can be approximately obtained:

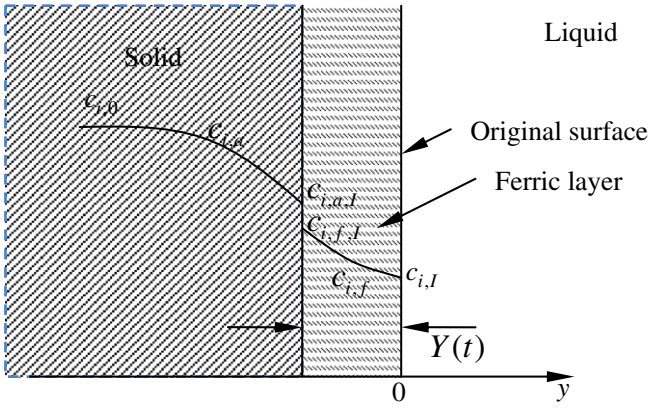

Fig. 7. Coordinate and concentration profile for the two-region problem without surface recession.

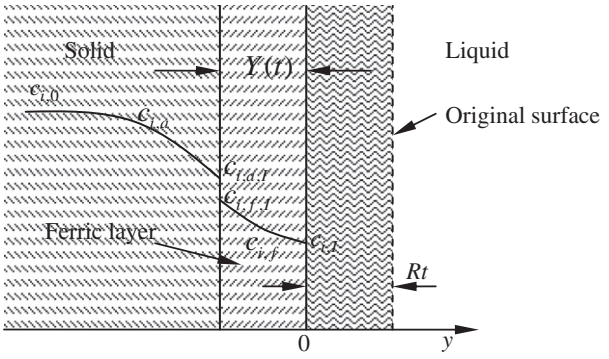

Fig. 8. Coordinate and concentration profile of the case with constant surface recession rate.

$$\frac{D_{Ni,f}(c_{Ni,I}-c_{Ni,f,I})}{Y_0}\approx R(c_{Ni,I}-c_{Ni,f,I}) \tag{130}$$

Because Y_0 is very small according to experimental result of steels exposure to liquid sodium. Then from Eqs. (129) and (130), it is easy to find:

$$k_p\approx D_{Ni,f} \tag{131}$$

which can be applied Eq. (129) to obtain the thickness of the ferric layer at the steady state. Then the species concentration in the ferrite and austenite can be obtained by:

$$c_{i,a}=c_{i,0}+(c_c-c_{i,0})\exp\left(\frac{R}{D_{i,a}}(y+Y_0)\right) \tag{132}$$

in austenite and

$$c_{i,f}=\frac{c_c-c_{i,I}\exp\left(-\frac{R}{D_{i,f}}Y_0\right)}{1-\exp\left(-\frac{R}{D_{i,f}}Y_0\right)}+\frac{c_{i,I}-c_c}{1-\exp\left(-\frac{R}{D_{i,f}}Y_0\right)}\times\exp\left(\frac{R}{D_{i,f}}y\right) \tag{133}$$

The concentration at the austenite/ferrite interface c_c is determined by Eq. (120a):

$$c_c=zc_{i,I}+(1-z)c_{i,0} \tag{134}$$

with $z=\exp\left(-\frac{R}{D_{i,f}}Y_0\right)$. Eq. (133) reduces to:

$$c_{i,f}=c_{i,0}-(c_{i,0}-c_{i,f})\exp\left(\frac{R}{D_{i,f}}(y+Y_0)\right) \tag{135}$$

Particularly, for nickel:

$$c_{Ni,I}=c_{Ni,0}-(c_{Nii,0}-c_{Ni,c})\exp(1) \tag{136}$$

If the nickel concentration at the liquid/solid interface is very small, i.e. $c_{Ni,I}\approx 0$, then one can estimate c_c by:

$$c_c=0.63c_{Ni,0} \tag{137}$$

The corrosion rate in term of weight loss can be obtained by:

$$J_{i,2}=\rho_s R c_{i,0} \tag{138}$$

6. Surface recession rate determination

Most of the existing coolant systems such as the primary nuclear coolant systems using liquid metals as coolants are made of stainless steels whose main component is iron. Considering that austenite/ferrite is a crystal consisting mainly of iron atoms, the loss of iron layer due to surface recession will release the other alloy elements contained in the crystal [28]. Therefore, it is reasonable to assume that it is the corrosion of iron that determines surface recession rate or the bulk corrosion rate. For highly leached species, the concentration in solid at the interface will be very low and can be assumed to be zero, while for slowly leached species, the concentration in solid at the interface will be a finite value which is larger than or equal its solubility in the liquid.

Considering that $J_{Fe,2}=J_{Fe,1}$ at the steady state, the recession rate can be obtained by:

$$R=\frac{1}{\rho_s c_{Ee,I}-\rho_L c'_{Fe,I}}\left(\rho_L D'_{Fe}\frac{\partial c'_{Fe}}{\partial \vec{N}}-\rho_S D_{Fe}\frac{\partial c_{Fe}}{\partial \vec{N}}\right) \tag{139}$$

For example, for the case of mass transfer control with two regions in solid and non-isothermal system, the surface recession rate can be obtained by equaling Eqs. (138) and (67):

$$R=\frac{0.3825\rho_L}{\rho_s c_{Fe,0}}\frac{D'_i}{d}\left(\frac{d}{L}\right)^{1/3}Sc^{1/3}\mathrm{Re}^{0.6}\sum_{k\neq 0}Q_k\exp(2\pi k i\xi) \tag{140}$$

in which the term $\rho_L c'_{Fe,I}$ is neglected considering that $c'_{Fe,I}\ll c_{Fe,0}$.

7. Oxygen effects on liquid metal corrosion

7.1. Oxygen solubility

Oxygen is the key impurity that affects the liquid metal corrosion. Commonly, for a light liquid metal (sodium and sodium–potassium alloy), the corrosion of iron based steels increases with the oxygen concentration in the liquid metal, while for a heavy liquid metal (lead and lead–bismuth alloy), the presence of oxygen may result in protective oxide layers that inhibit the corrosion.

The dissolution of oxygen into liquid metal is due to the following chemical reaction:

$$1/2\mathrm{O}_2(\mathrm{gas})=[\mathrm{O}](\mathrm{liquid})$$

According to Sieverts' law and if pure O_2 at 1 atmosphere is used as the standard reference, the oxygen partial pressure (p_{O_2}) in gas phase and the activity of oxygen dissolved in the liquid ($a_{[O]}$) can be related by:

$$p_{\mathrm{O}_2}^{1/2}(\mathrm{gas})=a_{[\mathrm{O}]}(\mathrm{liquid})=\gamma_{\mathrm{O}}X_{\mathrm{O}} \tag{141}$$

where X_O is the concentration of the oxygen atom in the liquid with a unit of mol fraction, and γ_O is the activity coefficient. The oxygen solubility in liquid metal has an expression as:

$$\log X_{O,s}=A+B/T \tag{142}$$

T is the temperature in K, A and B are constant. Values by measurement can be found in reference, for example, Ref. [29] for liquid sodium and sodium–potassium alloy, and Ref. [17] for liquid lead and lead–bismuth. The saturation partial pressure is related to the Gibbs energy of the formation of the liquid metal oxide through the following reaction:

$$xM+\frac{y}{2}\mathrm{O}_2=M_xO_y$$

where M is the liquid metal. The Gibbs energy can be expressed by:

$$\Delta G_{ox}=-RT\ln\left(\frac{a_{M_xO_y}}{p_{\mathrm{O}_2}^{y/2}a_M^x}\right) \tag{143}$$

Considering that the oxide is solid ($a_{M_xO_y}=1$), the saturation oxygen partial pressure can be expressed by:

$$p_{\mathrm{O}_2,s}^{1/2}=\frac{1}{a_M^{x/y}}\exp\left(\frac{\Delta G_{ox}}{yRT}\right) \tag{144}$$

Then for given oxygen concentration, the oxygen partial pressure can be obtained:

$$p_{\mathrm{O}_2}^{1/2}=\frac{X_O}{X_{O,s}}p_{\mathrm{O}_2,s}^{1/2} \tag{145}$$

The oxygen chemical potential is defined by:

$$\mu_{M,O}=RT\ln p_{\mathrm{O}_2} \tag{146}$$

7.2. Oxygen distribution coefficient

The oxygen dissolved in the liquid can be redistributed between the liquid metal and structural materials. The redistribution process won't stop until the oxygen chemical potentials in both phases (solid and liquid) equal each other, i.e. $\mu_{L,O_2}=\mu_{M,O_2}$. The diffusion coefficient $K_{D,O}$ is defined by:

$$K_D = \frac{X_O}{X'_O} = \frac{X_{O,s}}{X'_{O,s}} \left(\frac{p'_{O_2}}{p_{O_2}}\right)^{1/2} \quad (147)$$

Considering that the oxygen solubility in metals depends on the Gibbs energy of the formation of the most stable oxide of the metal, the oxygen distribution coefficient can be related to the Gibbs energy. As indicated by Smith and Natesan [30] the oxygen distribution coefficient can be expressed by:

$$\ln K_D = A + \frac{B}{T} \quad (148)$$

where A and B are constant. Values of A and B for kinds of pure solid metals in sodium and sodium–potassium are given in Ref. [29]. No data has been reported for the oxygen distribution coefficient between solid metals and liquid lead and lead–bismuth, however, as shown by Li [31] it is much easier to form stable oxide of the components of common stainless steel such as Fe, Cr and Ni than that of lead and bismuth.

The oxygen distribution coefficient is an important parameter that determines the oxygen effect on liquid metal corrosion. The larger the value is, the more easily the metal in the liquid will be oxidized. Therefore, based on the oxygen distribution coefficient values the materials for oxygen getter (in liquid sodium and NaK) and for protective oxide layer (in liquid lead and LBE) can be determined. The threshold oxygen level in the liquid metal/alloy for formation of stable oxide of the solid metal can be calculated through calculation of the oxygen distribution coefficient and the expression is:

$$\ln X'_O = \ln X_{O,s} - \ln K_D \quad (149)$$

X'_O is the threshold oxygen concentration.

7.3. Oxygen effects on corrosion by liquid sodium and NaK

The oxygen redistribution coefficients of Fe, Cr and Ni in liquid sodium and NaK are very small [29], which indicates that it is more difficult to form solid stable oxide of such metals than sodium and potassium. However, soluble ternary oxide can be formed in the form of $FeO{\cdot}nNa_2O$, so the solution of iron in liquid sodium can be increased by dissolved oxygen [32]. The oxygen-dependent iron solution in liquid sodium was given by Polley and Skyrme [33]:

$$c'_{Fe,s}\ (\text{ppm}) = c'^{1.45}_O 10^{-0.89-2347/T} \quad (150)$$

Eq. (150) indicates that the iron solubility in sodium increases with the dissolved oxygen concentration. There is an upper limit of iron solubility which is thought to be the iron solution in liquid sodium saturated with oxygen [4]:

$$c'_{Fe,s}\ (\text{ppm}) = 10^{1.804-842/T} \quad (151)$$

The metallic solution which is thought to be the low limit of Eq. (150) (the iron solution in sodium free of oxygen) was given by Baus et al. [34]:

$$c'_{Fe,s}\ (\text{ppm}) = 2.28 \times 10^{-3} - 1.63 \times 10^{-5} T\ (^\circ\text{C}) + 5.63 \times 10^{-8} T^2\ (^\circ\text{C}) \quad (152)$$

Eq. (151) determines the up limit of the iron solution while Eq. (152) determines the low limit with changing the oxygen concentration in the liquid metal. Eqs. (150)–(152) indicates that the iron solubility in liquid sodium depends strongly on the oxygen concentration in the liquid. For example, at 500 °C, the iron solubility in liquid sodium is about 0.008 ppm if the liquid is free of oxygen, while the concentration can increase to its up limit of 5.18 ppm with increasing the oxygen concentration.

Corrosion rate of steels in liquid sodium also depends on the oxygen concentration. Correlations between the corrosion rate and oxygen concentration in liquid sodium have been developed based on theoretical analyses or experimental data. They were summarized by Fidler and Collins in a review paper [35].

7.4. Oxygen effects on corrosion by liquid lead and LBE

The oxygen potential for forming lead and bismuth oxides is much higher than that for forming iron and chrome oxides [31]. Then in a liquid lead or LBE system, oxygen can act as a corrosion inhibitor though forming protective oxide layer on the steel surface. However, the oxygen level in the liquid needs to be carefully controlled to avoid heavy oxidation of the steel and precipitation of lead and bismuth oxides. Once the protective layer forms, the steel is separated from the liquid metal and directly dissolution is inhibited. The liquid metal corrosion appears as the dissociation of the protective layer, which is much lower than directly dissolution. Theoretical analysis [2] and experimental data [36] have shown that the corrosion rate by liquid lead and LBE decreases significantly with oxygen concentration increasing in a reasonable range.

Assuming that the protective layer is composed of Fe_3O_4, correlations for the corrosion rate of steels in flowing liquid lead and LBE have been developed theoretically [37]. In LBE, the correlation is expressed by:

$$R(m/s) = 0.014 V^{0.875} d^{-0.125} C'^{-4/3}_O (1-\alpha) \exp\left(\frac{-2,84,310}{RT}\right) \quad (153)$$

and in liquid lead, the correlation becomes:

$$R(m/s) = 0.434 V^{0.875} d^{-0.125} C'^{-4/3}_O (1-\alpha) \exp\left(\frac{-3,05,797}{RT}\right) \quad (154)$$

where the parameter α is the ratio of Fe concentration in the bulk liquid to the concentration at the oxide/liquid interface. Eqs. (153) and (154) show that the oxygen concentration has a power of $-4/3$ which indicates that the corrosion rate decreases with increasing the oxygen concentration in the liquid metal/alloy.

8. Models of corrosion–oxidation interactions in liquid lead and LBE with oxygen control

Using oxygen control technique has been found to be the most effective way to mitigate the corrosion of steel in liquid lead and LBE technology for coolant in advanced liquid lead or lead–bismuth alloy cooled nuclear reactors [38]. Corrosion–oxidation interactions at the steel surfaces are under wide-ranging investigation to understand the compatibility between steels and liquid lead/LBE. Experimental studies were reviewed [36], and this section focuses on the modeling studies.

Because of scatted test data and wide-ranging operation conditions, modeling of the corrosion–oxidation interactions of steel in liquid lead and bismuth becomes urgently necessary. The initial study on modeling of corrosion was carried out by He and Li [2] who developed an initial kinetic model to study the corrosion and precipitation rate in a non-isothermal LBE loop. Following this initial work, Zhang and Li illustrated the oxidation mechanisms [39] of steel in liquid lead and LBE and analyzed the corrosion–oxidation interactions [37]. Modeling studies were also carried out by European groups such as Steiner [40] and Martinelli et al. [41].

Assuming that there are two competitive processes going on simultaneously at the oxide/liquid interface, Zhang and Li employed the original Tedmon's model to interpret the corrosion–oxidation interactions [37] in liquid lead and LBE. The growth of the oxide layer is governed by the following equation:

$$\frac{d\delta_O}{dt} = K_O - R_O \tag{155}$$

where δ_O is the oxide layer thickness, K_O is the oxide layer growth rate and R_O is the scale removal rate. K_O depends on the oxygen potential in the liquid and the steel compositions, while R_O depends on the oxide layer compositions and flow conditions. It is reasonable to assume that R_O is constant for a steady state flow condition. Assuming the oxidation process follows the parabolic law with a parabolic constant $k_{p,O}$, a solution of Eq. (155) was given [42]:

$$\tau = -X - \ln(1 - X) \tag{156}$$

where τ and X are dimensionless time and oxide thickness defined by $\tau = tR_O/\delta_{O,f}$ and $X = \delta_O/\delta_{O,f}$ with $\delta_{O,f}$ is the asymptotic thickness having an expression:

$$\delta_{O,f} = \frac{k_{p,O}}{2R_O} \tag{157}$$

For early stages, the approximate solution becomes [43]:

$$X(\tau \to 0) = (2\tau)^{1/2} - \frac{2}{3}\tau \tag{158}$$

Eq. (158) has been applied to fit short-term (several thousand hours) experimental data. $k_{p,O}$ and R_O of kinds of steels under different operation conditions were reported [37].

Knowing the oxide layer growth rate, the weight change rate per unit area can be expressed in a non-dimensional formation as [42]:

$$R_w = f_O \frac{dX}{d\tau} - (1 - f_O) \tag{159}$$

where f_O is the mass fraction of the oxygen in the oxide.

Typical variations of the oxide (Fe_3O_4) layer thickness and the weight change of steel in flowing liquid lead and LBE are shown in Fig. 9. The layer thickness approaches its asymptotic value with time, while the weight first increases then it decreases with time after the peak. It is necessary to point out that the asymptotic thickness may not be reached because of periodic spallation of the unstable oxide layer.

Steiner [40] developed another equation to estimate the oxide removal by liquid lead and LBE:

$$\Delta_{loss}(t) = (\Delta_{recess}(t) - \delta_{i.o.z}(t))\Phi - \delta(t) \tag{160}$$

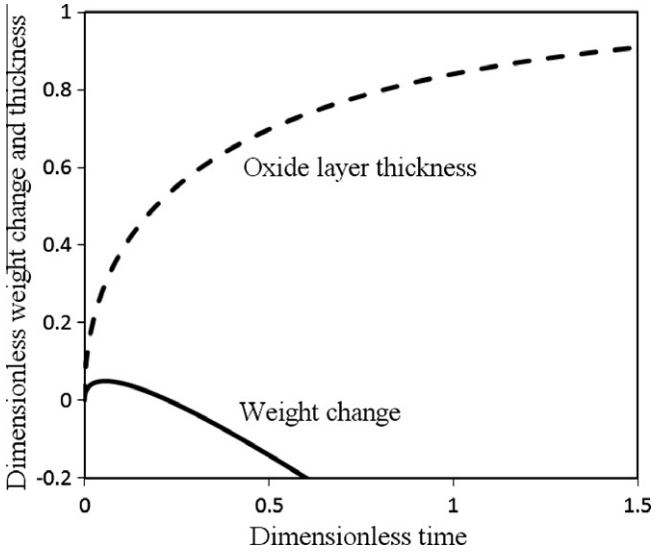

Fig. 9. Typical variation of oxide layer thickness and corresponding weight change of steel in flowing liquid lead and LBE.

where Φ is the Pilling–Bedworth ratio, Δ_{recess} is the metal recession and $\delta_{i.o.z}$ is the inner oxide zone. The equation was developed based on measured data of metal recession and oxide layer thickness. The model has been applied to T91 steel at a tested condition of temperature 550 °C, a flow velocity 0.5 m/s and an oxygen concentration 0.01 ppm. The scale loss (corrosion rate) was calculated to be in the range of 0–5 μm per year which is much smaller than the value calculated using Eq. (158) (Ref. 36).

9. Discussions

Compared with corrosion by aqueous solution which is known as an electro-chemical process, the corrosion by liquid metal does not involve electron transfer in the liquid and can be recognized as a physical–chemical process. Some models of liquid metal corrosion were developed based on mass transport in the solid phase, while others were based on mass transfer in the liquid phase. In the present survey, the two kinds of models were coupled through mass exchange at the solid/liquid interface to determine the bulk corrosion rate or the solid surface recession rate. For each kind of model, deferent solutions were presented for different operating conditions and assumptions, however, in the present study, the application ranges of each solution were not determined.

Corrosion models presented have been applied to study corrosion in the primary coolant loop in nuclear reactors and compared with experimental data to determine the model application ranges by different authors. Most of the studies agree with each other, while some studies result in contradict conclusions. Epstein [3] concluded that the corrosion by liquid sodium and sodium–potassium was more closely to activation control than to mass transfer based on comparisons between his model results and experimental data available, while by applying the kinetic model to analyze the same experimental data, Zhang et al. [4] believed that the corrosion is in the mass transfer control range. It is difficult to determine which calculation is better because both of the models need exactly operating conditions of the experiments which were not given in the original reference.

As discussed in Ref. [12], the activation controlled corrosion occurs when the flow velocity is high enough. Such cases should be excluded in a nuclear reactor design because high flow velocity can result in unexpected mechanical erosion. By assuming the corrosion is controlled by mass transfer in the liquid phase, comparisons between the results of Epstein's model, the Sannier and Santarini's model and the kinetic model were made in Ref. [17]. It was reported that the three models agreed with each other very well. Epstein's model is simple to be applied but can only predict the constant corrosion rate at the hottest section in a non-isothermal loop. It is assumed that the bulk concentration equals to the surface equilibrium concentration at the lowest temperature section, which results in a high corrosion rate because the bulk concentration is almost the average surface concentration all through the loop which is greater than the surface concentration at the coldest section [18]. The other two corrosion models can predict the downstream effects and the corrosion/precipitation zones. They are both based on the factor that the total amount corrosion equals to the total amount of precipitation all through the loop. Compared with Sannier and Santarini's model, the kinetic model is more complex to be applied, while the Sannier and Santarini's model needs more assumptions. It should be necessary to notice that all calculations in Ref. [17] did not consider the corrosion flux in the liquid phase due to recession of the surface as indicated in Eq. (6) (the second term on the right side).

Most of the model developments based on transport in solid phase are for sodium corrosion. The constituent distributions in the solid phases were analyzed in Refs. [33,25]. By comparisons

with experimental data, Anno and Walowit [25] believed that the two-region model can predict the thickness of the ferric layer with experimental errors.

Base on analysis of the transient model, the time for the transient process of the transport in liquid phases (several seconds) is very short compared with a reactor operation period. It is reasonable to consider only corrosion at the steady state in the liquid phase. In mass transfer control range, the boundary conditions for the transport in the liquid phase are constant concentrations, while the boundary conditions for the transport in the solid phase are constant fluxes which are obtained by solving the transport in the liquid phase. While in the activation control range, the concentrations at the solid/liquid interface in the solid side are constant, while fluxes into the liquid which is obtained by solving the mass transport equations in the solid phase are constant, and serve as boundary conditions for the transport in the liquid phase.

Through coupling each other at the interface, the transport in the solid can be applied to predict the constituent distribution change by corrosion in the solid phase, and the transport in liquid can predict the surface recession rate.

If the constants in the models are not available, they can be estimated by fitting experimental data using the some simplified solution. For example, the bulk corrosion rate and the parabolic oxidation constant in the oxidation–corrosion interaction model (Eq. (55)) were obtained by fitting the measured oxide layer thickness using the short-term solution (Eq. (158)). Then the long term interactions between corrosion and oxidation in an LBE system can be predicted using the model.

10. Conclusions

The modeling system set up in the survey can calculate the corrosion rate, corrosion layer thickness including the ferric layer due to selective corrosion and oxidation layer due to oxygen control, and transport of the corrosion product in both liquid and solid phases. The interactions between the liquid and solid and the oxygen effects are incorporated. The modeling system is expected to be applied to advanced nuclear reactor coolant systems using liquid metal as coolant such as liquid sodium, sodium–potassium, lead and lead–bismuth. Unfortunately, the pitting corrosion, stress corrosion cracking and liquid metal embrittlement and penetration corrosion are not included in the survey because of the scarce studies both experimental and theoretical. However, the degradation of structural materials by these kinds of corrosion has to be mitigated when operating a liquid metal coolant loop in an advanced reactor. Therefore, further experimental studies and realizable models need to be developed.

Acknowledgements

The author is grateful to Dr. N. Li at the Los Alamos National Laboratory and Dr. A. Hechanova at the University of Navada at Las Vegas for the initial support of this study.

References

[1] J.R. Distefano, E.e. Hoffman, Atomic Energy Review 2 (1964) 3–33.
[2] X. He, N. Li, Journal of Nuclear Materials 297 (2001) 214–219.
[3] L.F. Epstein, Liquid Metal Technology 20 (1957) 67–81.
[4] J. Zhang, T. Marcille, R. Kapernick, Corrosion 64 (2008) 563–573.
[5] J. Zhang, N. Li, Y. Chen, Nuclear Science and Engineering 154 (2006) 223–232.
[6] M.V. Polley, G. Skyrme, Journal of Nuclear Materials 66 (1977) 221–235.
[7] W.V. Pinczewski, S. Sideman, Chemical Engineering Science 29 (1974) 1969–1976.
[8] F. Berger, K.F.F.L. Hau, International Journal of Heat and Mass Transfer 20 (1977) 1185–1194.
[9] D.C. Silverman, Corrosion 40 (1984) 220–226.
[10] P. Harriott, R.M. Hamilton, Chemical Engineering Science 20 (1965) 1073–1078.
[11] L.F. Epstein, Science 112 (1950) 426.
[12] F. Balbaud-Celerier, F. Barbier, Journal of Nuclear Materials 289 (2001) 227–242.
[13] M. Soliman, P.L. Chambre, International Journal of Heat and Mass Transfer 10 (1967) 169–180.
[14] J. Zhang, N. Li, Journal of Nuclear Materials 321 (2003) 184–191.
[15] A. Vary, A semiemplirical model for boundary layer diffusion in forced convection flow, NASA Technical Note, NASA TN D-7012, 1970.
[16] J. Sannier, G. Santarin, Journal of Nuclear Materials 107 (1982) 196–217.
[17] J. Zhang, N. Li, Journal of Nuclear Materials 373 (2008) 351–377.
[18] J. Zhang, N. Li, Nuclear Technology 144 (2003) 379–387.
[19] H. Steiner, J. Konys, Journal of Nuclear Materials 348 (2006) 18–25.
[20] S.J. Wachtel, A.J. Romano, C.J. Klamut, H.S. Isaacs, J.R. Weeks, D.H. Gurinsky, Chemical aspects of corrosion and mass transfer in sodium, in: AIME Symposium, Detroit, 1971, p. 232.
[21] J. Weeks, H.S. Isaacs, Corrosion and deposition of steels and nickel-based alloys in liquid sodium, in: M.G. Fontana, R.W. Staehle (Eds.), Advanced in Corrosion Science and Technology, vol. 3, 1973, pp. 1–67, p. 45.
[22] L.M. Skinner, J.R. Sambles, Journal of Aerosol Science 3 (1972) 199–210.
[23] E.G. Brush, Sodium mass transfer XVI: the selective corrosion component of steel exposed to flowing sodium, GEAP-4832, 1965.
[24] J.R. Weeks, H.S. Isaacs, Corrosion and deposition of steels and nickel-base alloys in liquid sodium, in: M.G. Fontana, R.W. Staehle (Eds.), Advanced in Corrosion Science and Technology, vol. 3, 1973, pp. 1–67, p. 17.
[25] J.N. Anno, J.A. Walowit, Nuclear Technology 10 (1971) 67–75.
[26] M.W. Polley, An analysis of the selective mass transfer of alloys exposed to flowing sodium, TD/B/N3624, General Electricity Generating Board, 1976.
[27] C.S. Tedmon Jr., Journal of the Electrochemical Society 113 (1966) 766–768.
[28] M. Schad, Nuclear Technology 50 (1980) 267–288.
[29] J. Zhang, R. Kapernick, Progress in Nuclear Energy 51 (2009) 614–623.
[30] D.L. Smith, K. Natesan, Nuclear Technology 22 (1974) 392–404.
[31] N. Li, Journal of Nuclear Materials 300 (2002) 73–81.
[32] J.D. Mottley, Sodium mass transfer VIII: corrosion of stainless steel in isothermal regions of a flowing sodium system, GEAP-4313, 1964.
[33] M.V. Polley, G. Skyrme, Journal of Nuclear Materials 66 (1977) 221–235.
[34] R.A. Baus, The solubility of structural materials in sodium, in: Proceeding of the International Conference on the Peaceful uses of Atomic Energy, Held in Geneva, August, 1955, vol. 9, United Nations Publications, New York, 1956.
[35] R.S. Fidler, M.J. Collins, Atomic Energy Review 13 (1975) 3–50.
[36] J. Zhang, Corrosion Science 51 (2009) 1207–1227.
[37] J. Zhang, N. Li, Corrosion Science 49 (2007) 4154–4184.
[38] N. Li, Progress in Nuclear Energy 50 (2008) 140–151.
[39] J. Zhang, N. Li, Oxidation of Metals 63 (2005) 353–381.
[40] H. Steiner, Journal of Nuclear Materials 383 (2009) 267–269.
[41] L. Martinelli, F. Balbaud-Celerier, G. Picard, G. santarini, Corrosion Science 50 (2008) 2549–2559.
[42] J. Zhang, N. Li, Y. Chen, Journal of Nuclear Materials 324 (2005) 1–7.
[43] H. Taimatsu, Journal of Electrochemica Society 146 (1999) 3686–3689.